JOURNAL OF PROPULSION AND POWER
Vol. 22, No. 4, July–August 2006

Measurements of Intake Separation Hysteresis in a Model Fan and Nacelle Rig

C. A. Hall* and T. P. Hynes†
University of Cambridge, Cambridge, England CB2 1PZ, United Kingdom

A 1/20-scale, low-speed model rig representing the fan and nacelle of a high-bypass-ratio jet engine has been tested in a range of simulated crosswinds. The flow conditions under which the intake flow separates and reattaches have been found to exhibit considerable hysteresis. This phenomenon has been examined by a careful test procedure in which the crosswind angle has been slowly increased and then decreased. Measurements of the hysteresis associated with separation and reattachment are presented for independent variations in stream-tube contraction ratio, ground clearance, fan operating point, and Reynolds number. The results reveal that particular care must be taken to allow for any hysteresis when testing intakes under crosswind conditions. They also indicate that separation hysteresis is particularly sensitive to fan operating point and the position of the ground plane. These findings suggest that it is important for high-Reynolds-number intake tests and calculations to include a ground plane and a model of the downstream turbomachinery.

Nomenclature

A	=	area
C_p	=	surface-pressure coefficient
D_1	=	intake highlight diameter
DC_{60}	=	total pressure distortion coefficient
h	=	height of the rig or engine centerline
L_q	=	size of the captured stream tube in the far field
$\dot{m}$	=	mass flow rate through the rig or engine
p, p_0	=	static pressure, stagnation pressure
Re	=	Reynolds number based on highlight diameter and the mean flow velocity entering the intake
r	=	radial coordinate measured from the rig centerline
V_∞	=	far-field characteristic mean wind speed
x	=	axial coordinate measured from the inlet highlight
Y_p	=	intake loss coefficient
α	=	wind direction relative to the rig centerline
θ	=	intake circumferential position
ρ	=	density
ϕ	=	flow coefficient (ratio of the mean axial-flow velocity to the mean blade speed)

Subscripts

f	=	fan parameter
HL	=	value at the nacelle highlight (the most forward point of the intake)
TH	=	value at the nacelle throat (the minimum flow area within the intake)
2	=	value at the fan face
∞	=	far-field value in the freestream

I. Introduction

THE intake of a jet engine is least tolerant to crosswind when it is operating statically and close to the ground. The flow drawn into the engine can separate from the inlet lip leading to nonuniform flow within the intake duct. This pushes the operating point of the fan towards instability, and, if the distortion is large enough, the fan might stall.

Freeman and Rowe[1] demonstrated that engine fan stall events could occur as a result of dynamic interaction between the atmospheric flow, the intake flowfield, and the fan aerodynamics. In other words, the response of an engine to natural wind cannot be determined from the steady performance of the intake when tested in isolation in a crosswind. These findings initiated a study aimed at improving our understanding of the behavior of a large turbofan engine operating close to the ground in natural wind, which is described in Hall.[2] A major conclusion from that study was that in order to understand the behavior of the intake in unsteady, natural wind conditions it is necessary to take account of the considerable hysteresis exhibited in the separation and reattachment of the flow into the intake as the wind angle changes. The present paper represents a detailed experimental investigation into separation hysteresis. The companion paper, Hall and Hynes,[3] uses the results presented here, in conjunction with measurements taken in unsteady flow, to develop a model of how an engine intake responds to atmospheric wind conditions.

There are many examples of hysteresis phenomena observed in fluid mechanics:

1) In the stalling of a compressor, the throttle opening required for stall is much greater than that needed for stall cessation.[4]

2) For an aerofoil operating at high angles of attack, the flow structure is ambiguous for a range of flow conditions.[5]

3) In the transonic flow past cylindrical bodies, there are regions of the flow that can be separated or attached depending on how the condition was approached.[6]

4) The conditions at which a thin jet is attached to an adjacent surface are not unique because the flowfield possesses some memory of the previous transients.[7]

In every example, the hysteresis leads to nonunique behavior, where a given set of boundary conditions is compatible with more than one solution. This has serious implications. It means that the state of a flowfield investigated using steady experiments or calculations can depend on how the steady condition is established. In terms of aerodynamic design, it is difficult to predict the extent of hysteresis and the variation of aerodynamic parameters around a hysteresis loop. Therefore, the design must eliminate the hysteresis or avoid any regions of nonunique behavior by ensuring that there can be no unfavorable transients.

At present there are few established theoretical bases for analyzing aerodynamic hysteresis, and it remains a difficult phenomenon to examine numerically. This is especially true of hysteresis phenomena associated with boundary-layer separation and reattachment. However, there have been several experimental studies, and

Presented as Paper 2002-3772 at the AIAA/ASME/SAE/ASEE 38th Joint Propulsion Conference & Exhibit, Indianapolis, IN, 7–10 July 2002; received 20 July 2005; revision received 8 December 2005; accepted for publication 12 December 2005.

*Research Associate, Department of Engineering, Trumpington Street. Member AIAA.

†Senior Lecturer, Department of Engineering, Trumpington Street.

these are considered further here as they were used to guide the experimental procedures described in the present paper.

Zanin[8] showed how separation hysteresis could be investigated using a wing mounted at a constant angle of attack with slow variations in the wind-tunnel speed. With the flow velocity increasing, flow reattachment starts at the edges of the wing and progresses inwards gradually as the flow speed rises. For the velocity decreasing, the flow remains completely attached for much longer than with the velocity increasing, and separation is restored rapidly over the entire wing surface. A similar phenomenon was observed in studying the hysteresis arising from varying the angle of attack. Instantaneous separation occurs with an increase in the angle of attack, and gradual reattachment is seen as the angle is reduced. Golovkin et al.[9] describe similar experiments with rectangular wing profiles in wind tunnels in which the angle of attack was increased slowly from 0 to 30 deg and then decreased from 30 deg back to 0 deg. Significant hysteresis was found in the measured coefficients of aerodynamic forces and moments with respect to the flow angle.

Guzhavin and Korobov[6] investigated the regions of attached and separated flow around bodies of revolution immersed in transonic flow. A series of experiments was performed that enabled the separation hysteresis to be expressed in terms of Mach number, flow angle, Reynolds number, and geometry. It was found that at supersonic velocities an important part is played by the formation and breakup of supercritical flow regions around the points of reattachment. The authors concluded, similarly to Horton,[10] that the origin of the hysteresis is the attainment of instability in the fluid flow and an abrupt changeover to a new stable state.

There is limited literature available relating to separation hysteresis in the flow entering engine intakes. Quemard et al.[11] indicate that large hysteresis effects can be observed when testing model intakes at varying angles of attack, and they describe measures that are taken to avoid any ambiguous results. Seddon and Goldsmith[12] state that there is significant hysteresis in the separation of an inlet at incidence, but there are no measurements presented that clearly show the separation and reattachment boundaries. The current paper aims to improve this situation by providing the first systematic study of intake separation hysteresis. It provides some insight into the physical mechanisms that are important to intake separation and reattachment and explores how the hysteresis varies with the relevant nondimensional parameters. It thus aims to make a contribution to the fields of engine intake aerodynamics and flow separation.

II. Experimental Method

Figure 1 is a photograph of the instrumented setup used for the investigation of inlet separation hysteresis. The rig scale, relative to a typical modern high-bypass-ratio turbofan, is nominally 1/20.

The fan unit used in the rig is a commercially available product that would normally be driven by a small internal combustion engine and mounted on a remote control model aircraft. In the current application, a high-speed motor drives the fan. The function of the fan is to provide the mass flow rate through the rig and, if possible, to reproduce features of the interaction between a full-scale engine fan and nacelle. A traversing throttle plate downstream of the stage controls the fan pressure ratio.

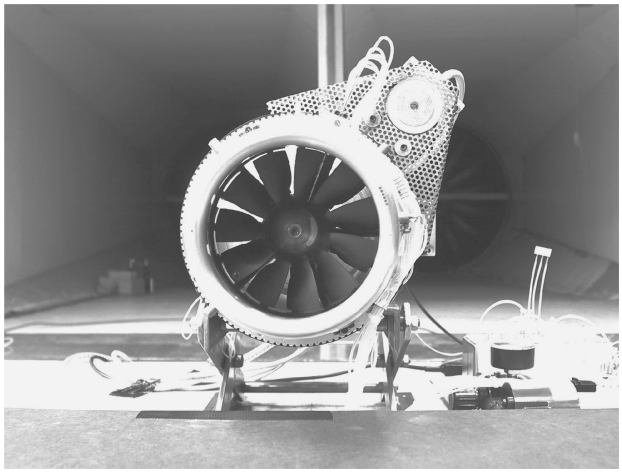

Fig. 1 Model fan and intake rig mounted above a ground plane in the Osney Laboratory environmental wind tunnel.

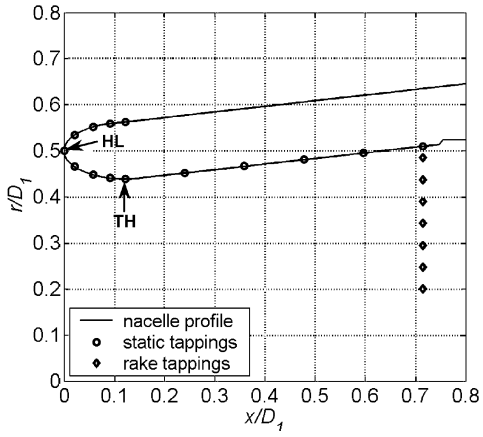

Fig. 2 Model intake geometry and the location of pressure tappings.

The model rig nacelle geometry and the location of the basic instrumentation are shown in Fig. 2. The inlet lip was designed to match the fan and to operate satisfactorily at the Reynolds number of the experiments. It was not practical to use a scaled-down engine nacelle because this would tend to be separated all of the time at low Reynolds numbers. As a result, the rig intake lip is much thicker, and the diffuser angle is lower. The geometry is axisymmetric, and it can be rotated, using a stepper-motor, through 360 deg enabling the internal flowfield to be surveyed.

All of the experiments were performed inside the environmental wind tunnel at the Osney Laboratory in Oxford. A complete description of the tunnel can be found in Wood.[13] The working section is 2 m high and 4 m wide. There is a 3.5 meter diameter wooden turntable, on which the model rig was mounted, that is rotated by a motor. Upstream of this, a length of 12 m is available to arrange turbulence generators for the simulation of atmospheric boundary layers. For the experiments in this paper, the tunnel was cleared except for the model rig and a raised wooden platform to simulate the ground (see Fig. 1).

The velocity field of the flow above the ground plane without the rig present was shown to be uniform with a streamwise turbulence intensity of less than 0.5%. This low level of unsteadiness was used for all of the experiments in the present paper. The effect of significant freestream turbulence on the intake flowfield is explored in the companion paper, Hall and Hynes,[3] when the turbulence generators were present.

Nondimensional Parameters and Test Procedure

For steady flow conditions in the wind tunnel, the flow-field within the model intake only depends on the nondimensional parameters shown on the right-hand-side of the following equation:

$$DC_{60} = f\{Re, \phi, L_q/D_1, \alpha, h/D_1\} \tag{1}$$

The distortion coefficient DC_{60} (defined later) is used to characterize the performance of the intake. For a full-scale engine this correlates with the effect of the intake flow on the stability of the fan, which is critical for operation within crosswind. However, DC_{60} could be replaced in Eq. (1) by any measure of the intake flowfield because the parameters on the right-hand side fix all of the flow characteristics. The following subsection shows how each of the parameters on the right-hand side of Eq. (1) can be set independently using the rig and wind-tunnel control systems. The experimental arrangement thus provides an ideal vehicle for the type of phenomena that are the topic of this paper.

Two types of experiments are detailed in this paper. The first are extensive steady flowfield measurements completed with the rig at a fixed operating condition. Once the parameters in Eq. (1) were set

Table 1 Summary of the experiment parameters and the uncertaintly in their measurement and control

Parameter	$Re = \dot{m}_f/\mu D_1$	$\phi_f = \dot{m}_f/\rho_\infty A_f U_f$	$L_q/D_1 = \sqrt{\dot{m}_f/\rho V_\infty D_1^2}$	α, deg	h/D_1
Typical engine values	2×10^7	0.5	2–5	0–180	0.80–1.20
Range of rig values	0–4 $\times$ 10^5	0.3–0.65	2–4	0–90	0.75–1.25
Uncertainty on rig values	±2%	±2%	±6%	±4	±0.5%

to the required experimental condition, the intake pressure field was traversed through 360 deg in 10-deg intervals. These tests show the details of the intake flowfield, as fixed by the terms in Eq. (1), and they are important to the current research because they demonstrate the presence of separation hysteresis and the need for a further study of this phenomenon.

The second type of experiment examines the hysteresis in the intake flowfield. The test procedure used is similar to that used by Golovkin et al.[9] for separation on a wing section: for an otherwise fixed steady operating condition, the crosswind angle was increased at a constant rate of 2 deg/s from 0 to 90 deg by rotating the turntable on which the rig was mounted. The flow angle was then reduced at the same rate until the flow was parallel with the rig centerline. This variation in wind direction is slow relative to any rig timescale, and therefore the test can be described as quasi steady.

Control and Uncertainty of the Experimental Variables

The control of the parameters on the right-hand side of Eq. (1) is of fundamental importance to the experimental results shown in this paper. The following paragraphs show how these parameters are adjusted independently, and estimates in the error associated with their measurement are presented.

The intake Reynolds number is defined using conditions at the highlight plane, $Re = \dot{m}_f/\mu D_1$, and is therefore independent of the wind speed. It determines the state and stability of the boundary layer on the nacelle surface, and it is the parameter that is most different in the experiments from the full-scale engine. It was carefully controlled in the experiments by setting the rig fan speed to give the desired rig mass flow once the throttle position had been fixed. The main uncertainty in the intake Reynolds number was caused by the error in rig mass flow calculated from the flow coefficient (see the following). The overall experimental error determined in the appendix is ±2%.

The flow coefficient, $\phi_f = \dot{m}_f/\rho_\infty A_f U_f$, fixes the model fan operating condition. For the incompressible conditions used in these experiments, ϕ_f is the only independent variable required to determine the mean flowfield within the fan. It was set using the rig throttle, which was accurately controlled via a stepper motor. This was much more convenient than measuring the rig mass flow for each experimental condition, and this approach is also more consistent with engine tests in which the nozzle exit area is adjusted to set the fan working line. The rig mass flow was calibrated against throttle position using a detailed radial traverse of a pitot tube in a uniform pipe section fitted upstream of the intake. This was repeated for the full range of throttle positions and fan speeds. The resulting error between the calibration and the true flow coefficient was estimated as ±2%. However, the level of repeatability between experiments should be much better than this because the throttle position was set to within ±0.1%.

L_q/D_1 is the stream-tube contraction ratio of the flow entering the intake. The parameter, $L_q = \sqrt{(\dot{m}/\rho_\infty V_\infty)}$, is the length scale of the capture stream tube in the far field, and this determines the geometry of the flow outside the intake: a small value represents a strong crosswind that is not greatly perturbed by the engine presence, whereas a large value represents a light crosswind that contracts strongly as it is drawn into the engine. The stream-tube contraction ratio is therefore the nondimensional group that accounts for the wind speed. Setting the wind-tunnel speed once the fan speed and the rig throttle position had been fixed allowed this to be controlled independently of intake Reynolds number and fan flow coefficient. The error in stream-tube contraction ratio is determined in the appendix to be ±6%.

The wind direction α has a large influence on the intake flowfield because it determines the distribution of lip loading around the circumference of the nacelle. Section II shows that as the local incidence angle increases the velocity at the highlight increases, and greater diffusion to the throat is required. It was set using the tunnel turntable and recorded by a potentiometer wind vane positioned on the turntable above the level of the rig. For each session of experiments, the wind vane was calibrated in situ against a protractor marked on the tunnel turntable. The accuracy in measured flow angle during the quasi-steady hysteresis tests was found to be ± 4 deg. However, in the steady flow measurements when the flow angle was set using the turntable protractor, the accuracy should be within ±0.5 deg.

The ground clearance distorts the shape of the approaching capture stream tube and determines whether an inlet vortex can form between the ground and the intake. The height of the metal frame that the rig was mounted on was adjustable, and the distance from the ground to the rig centerline was simply measured with a ruler. This was estimated to give an uncertainty in h/D_1 of less than $\pm 0.5\%$.

Table 1 summarizes the experimental variables, showing the range of values that could be achieved in the tests and comparing these with typical full-scale values for a modern civil turbofan engine.

III. Steady Flowfield Measurements

An exhaustive study of the intake steady flowfield is presented in Hall.[2] The results shown in this section were all obtained with the following datum values of experimental variables: $h/D_1 = 1$, $L_q/D_1 = 3$, $Re = 3 \times 10^5$, and $\phi = 0.62$. In terms of ground clearance, stream-tube contraction ratio, and wind direction, these conditions are typical of a modern wing-mounted jet engine operating in crosswind. These datum parameters were also chosen so that the fan would be well clear of stall (even with the intake separated) and so that the dependency of the results on Reynolds number would be weak. The suitability of the datum values is demonstrated by the hysteresis results shown later.

The aims of this section are to show that the intake measurements clearly show the flow features that lead to intake separation and to demonstrate the existence of nonunique behavior in the flowfield. These findings are the basis of the following detailed investigation of intake separation hysteresis.

Surface Pressure

The surface-pressure field is the main indicator of how the nacelle responds to the external flow conditions. Separation of the flow from the intake lip is expected when the local pressure gradient becomes too high.

The surface-pressure coefficient for the nacelle static pressure tappings is defined as follows:

$$C_P = \frac{p_{0\infty} - p}{p_{0\infty} - p_{\mathrm{TH}}} \tag{2}$$

The circumferentially averaged static pressure at the nacelle throat p_{TH} is used as the reference static pressure because this is measured accurately and it remains relatively constant for a given intake Reynolds number. Figures 3a–3c show plots of pressure coefficient measured around the circumference of the nacelle for the pressure tappings at the highlight, the peak suction point, the throat, and three positions along the diffuser duct. The nacelle circumferential position is measured clockwise from the top dead center looking into the rig. With the wind at an angle to the intake, the

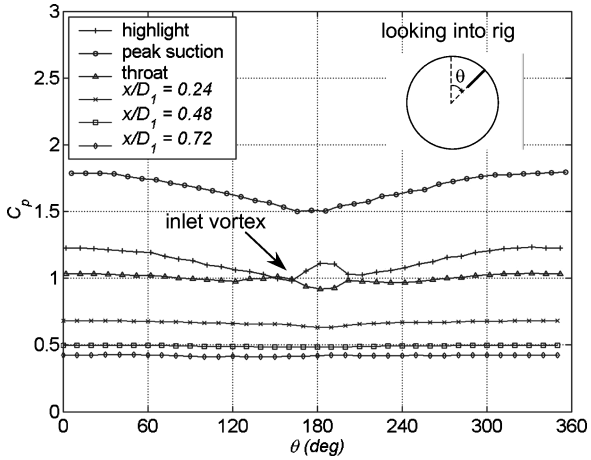

Fig. 3a Nacelle surface static pressure for $\alpha = 0$ deg.

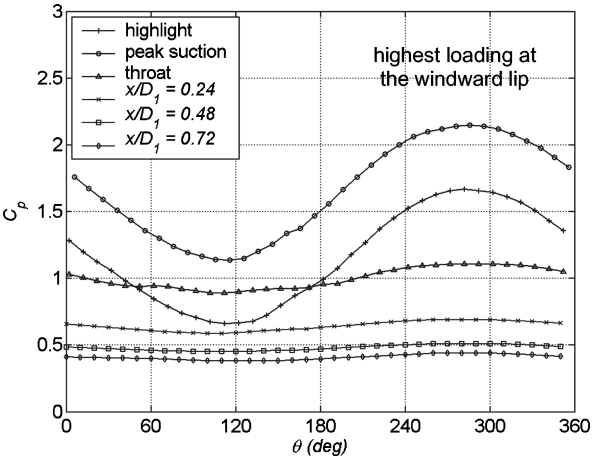

Fig. 3b Nacelle surface static pressure for $\alpha = 45$ deg.

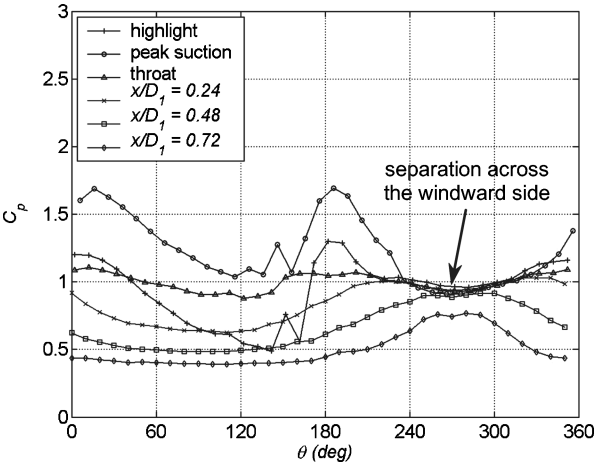

Fig. 3c Nacelle surface static pressure for $\alpha = 60$ deg.

most windward point is at 270 deg, and the most leeward point is at 90 deg.

Figure 3a shows the surface-pressure distribution with the wind parallel to the rig centerline. The presence of the ground causes more flow to be drawn from above the intake than below leading to higher aerodynamic loading at the top lip. This effect is also shown in numerical predictions such as Nangia and Palmer.[14] There are perturbations in the lip pressure distributions near to the bottom of the intake that can be attributed to the presence of an inlet vortex. As the wind direction increases, the circumferential variation in pressure coefficient increases. Figure 3b shows the surface-static-pressure distribution for a 45-deg crosswind with the inlet flow attached. The aerodynamic loading of the intake lip follows an almost sinusoidal variation, which is consistent with the change in momentum required to turn the incoming wind to the axial direction. Figure 3c shows the surface-static-pressure distribution once the intake flow has separated. Along the windward surface of the nacelle, the measured pressures collapse to an almost constant value. High aerodynamic loading occurs at the top and bottom of the nacelle where the flow remains attached, and there is still significant loading from the local incidence of the flow onto the intake.

Intake Performance

The loss coefficient for a sector of the intake is defined as follows:

$$Y_P = \frac{(p_{0\infty} - p_{02})_\theta}{p_{02} - p_2} \tag{3}$$

where $(p_{0\infty} - p_{02})_\theta$ is the area weighted average loss in total pressure for the sector considered and $p_{02} - p_2$ is the area-averaged dynamic head at entry to the fan. The choice of area, rather than mass, weighting is driven by our ultimate interest in fan stability issues rather than installed performance. The positions of the rake pressure tappings, as shown in Fig. 2, were optimized to look at separated flow and are therefore inadequate for measuring the details of the intake boundary layer. Indeed, attached boundary layers will appear unrealistically thick with this arrangement. The uncertainty in the measurement of loss coefficient is further exacerbated by the fact that the pitot tubes are not necessarily aligned with the flow direction. This was estimated to give an overall error of $\pm 5\%$ in local total pressure measurement.

Figures 4a and 4b show contours of measured loss coefficient for the rig operating at identical experimental conditions. In the first case, Fig. 4a, the far-field wind angle was being increased between each traverse of the intake. For Fig. 4b, the flow had already separated, and the wind angle was being decreased between each traverse. The differences between the figures are surprising. They

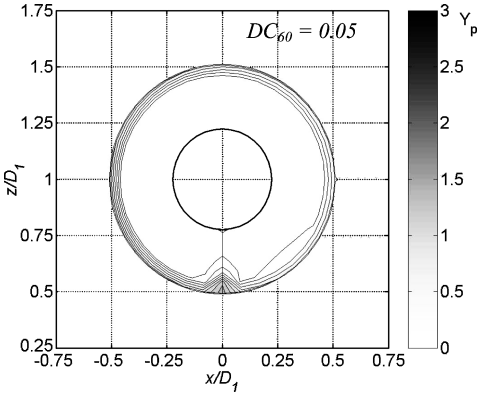

Fig. 4a Contours of loss coefficient with the intake flow attached; $\alpha = 45$ deg.

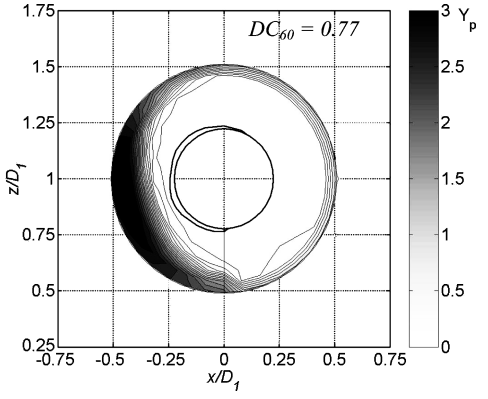

Fig. 4b Contours of loss coefficient with the intake flow separated; $\alpha = 45$ deg.

reveal that the performance of the intake for a given operating point is not unique and that separation hysteresis has a significant effect on the measurements.

With the intake flow attached, the greatest loss occurs near to the bottom of the annulus where the ground vortex is ingested. Once the intake flow separates, the flow approaching the fan becomes highly nonuniform. Although the shape of the separated region is three dimensional, it was found to be highly repeatable between tests.

The distortion coefficient for the model intake is defined as

$$DC_{60} = \frac{p_{02} - p_{02,60}}{p_{02} - p_2} \tag{4}$$

where p_{02} and p_2 are the area weighted average total and static pressures at the fan face and $p_{02,60}$ is the area averaged total pressure for the 60-deg segment with the lowest mean total pressure.

For the case with the flow attached, the level of distortion, $DC_{60} = 0.05$, would be acceptable for an engine fan, whereas the value with the flow separated, $DC_{60} = 0.77$, would be unacceptable. This indicates the importance of knowing the state of the inlet flow and in understanding the separation hysteresis.

IV. Quasi-Steady Measurements

Using the quasi-steady test procedure described earlier, separation hysteresis can be examined in terms of the variation of the aerodynamic parameters C_p and DC_{60}. This procedure, despite the unpredictability of flow separation, was found to be remarkably repeatable, and it was clear when the flow was attached and when it was separated. These observations are demonstrated by Fig. 5, which follows the variation in aerodynamic lip loading with wind direction for three separate tests performed with identical operating conditions. The aerodynamic lip loading used is defined as loading $= (V_{HL} - V_{TH})/V_{HL}$.

Figure 5 shows that below a particular wind direction the reattachment angle, the intake flow is always attached. For wind directions greater than the separation angle, the intake is always separated. The hysteresis region lies between these two critical directions, and within this range the flowfield can exist in one of two distinct states.

Intake Performance Variations

Figure 6a follows the variation in the pressure coefficient at the highlight of the windward lip. Results are shown for three values of stream-tube contraction ratio L_q/D_1. For small crosswind angles, as the size of the capture stream tube increases, the flow approaching the inlet stagnates further back from the highlight. This leads to greater acceleration around the highlight and higher aerodynamic loading. The rate of increase of pressure coefficient with wind direction increases with decreasing L_q/D_1. This is expected because a lower value of L_q/D_1 corresponds to a higher wind speed. The pressure coefficient at the point of separation is similar for all three cases, and this suggests that the inlet flow separates once a critical level of aerodynamic loading is exceeded. Although the results are

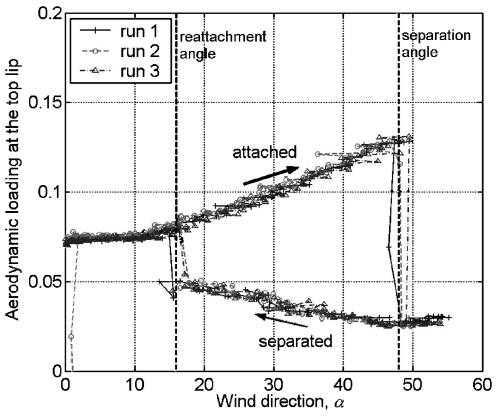

Fig. 5 Repeatability of the hysteresis tests: $h/D_1 = 1$, $L_q/D_1 = 3$, $Re = 3 \times 10^5$, and $\phi = 0.62$.

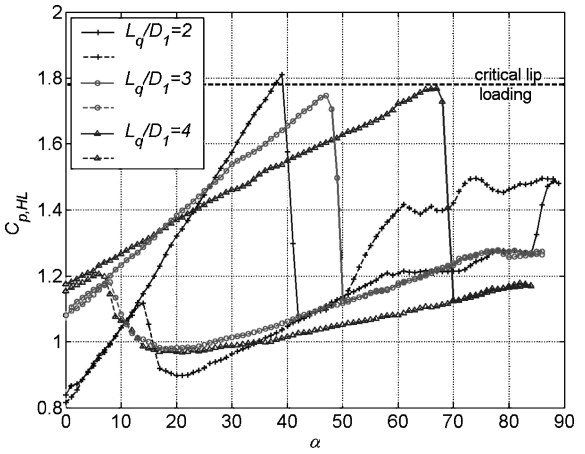

Fig. 6a Variation of pressure coefficient at the windward lip highlight: $h/D_1 = 1$, $Re = 3 \times 10^5$, and $\phi = 0.62$.

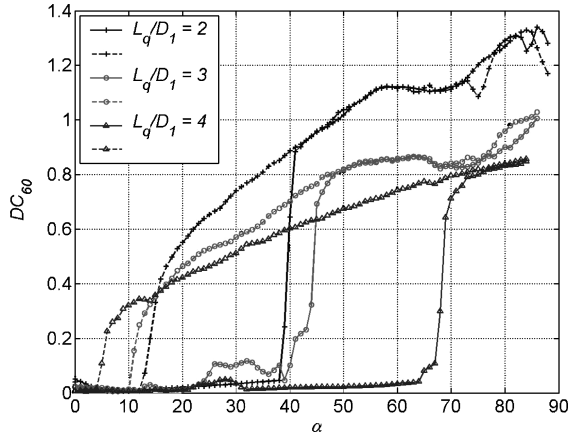

Fig. 6b Variation of intake distortion coefficient: $h/D_1 = 1$, $Re = 3 \times 10^5$, and $\phi = 0.62$.

not presented here, the same level of critical loading was found to apply for a large number of experiments, Hall.[2]

The separated part of the hysteresis loop also has some regular features. The rate of increase of pressure coefficient with far-field angle is reduced when the flow is separated, but it still decreases with stream-tube contraction ratio. In all cases the minimum pressure coefficient occurs close to $\alpha = 20$ deg, and a region where the rate of change of pressure coefficient with angle becomes negative precedes reattachment. The study of aerofoil dynamic stall in McCroskey et al.[15] suggests that this might be relevant to the reattachment process, but further measurements are needed to examine the mechanism further. In all cases, reattachment returns the flow to attached operation at an almost identical condition to that measured with the angle increasing.

Figure 6b shows the variation of distortion coefficient for the same experimental conditions investigated in Fig. 6a. To measure the distortion coefficient, the quasi-steady variation in wind direction was repeated eight times with the inlet rake at different circumferential positions. The plot shows that there is very little distortion whenever the flow is attached and that the flow separates later as the stream-tube contraction increases. When separated, the distortion is highest for low stream-tube contraction, as expected, and it increases with further angle increases. The separated distortion curves are smooth, continuous functions, and before reattachment the measured distortion is much lower than the distortion just after separation.

Hysteresis Maps

The measurements from hysteresis tests can be reduced to simple plots that show the variation of the experimental conditions on the separation and reattachment points. A comprehensive matrix of tests covering a wide range of values of each of the experimental variables

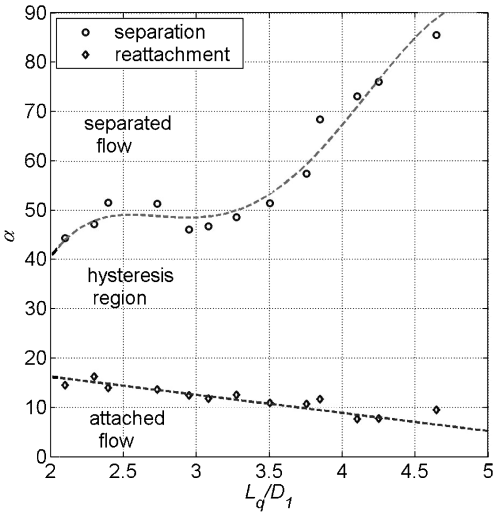

Fig. 7 Hysteresis map showing the effect of stream-tube contraction ratio: $h/D_1 = 1$, $Re = 3 \times 10^5$, and $\phi = 0.62$.

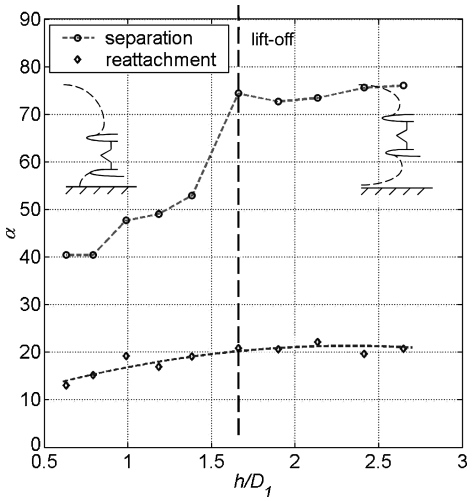

Fig. 8 Hysteresis map showing the effect of ground clearance: $L_q/D_1 = 3$, $Re = 3 \times 10^5$, and $\phi = 0.62$.

was completed. The results of these tests are summarized in this section, and they represent, to our knowledge, the most complete study of intake separation hysteresis to date.

Figure 7 summarizes a series of hysteresis tests in which the stream-tube contraction ratio has been changed between each quasi-steady variation in the wind direction. For each test all of the other experimental variables are held fixed, and the separation and reattachment angles are found automatically from the angles where the lip static-pressure field changes most rapidly. Polynomials have been fitted to the measured separation and reattachment points to mark the boundaries between the different flow regimes. These polynomials are applied in Hall and Hynes[3] to define criteria for separation and reattachment.

The results in Fig. 7 show that the wind direction required for separation is fairly constant until the stream-tube contraction ratio exceeds about 3.5. Above this value the separation angle increases rapidly with increasing L_q/D_1. This is consistent with the results in Fig. 6a. The measurements also show that as the stream-tube contraction increases the reattachment angle reduces. Hence, the overall amount of separation hysteresis increases with stream-tube contraction ratio.

Figure 8 shows the effect of ground clearance on the separation and reattachment boundaries. For nondimensional ground clearances up to about 1.5, the wind direction required for separation increases with h/D_1. This is expected because the aerodynamic lip loading is increased by the ground proximity. Between ground clearance values of 1.5 and 1.7, there is a sudden rise in the separation angle. This corresponds to the point where the captured stream tube lifts off the ground plane completely, and this condition was investigated with flow visualization using smoke. The flow entering the inlet was seen to not make contact with the ground plane if the captured stream-tube radius in the far field was less than the centerline height of the rig, that is, if the following were true:

$$h/D_1 \geq \left(1/\sqrt{\pi}\right)(L_q/D_1) \tag{5}$$

From the results in Fig. 8, it appears that the ground has negligible influence on the flowfield once the inequality in Eq. (5) is satisfied. However, modern wing-mounted jet engines have a value of ground clearance in the range $0.75 < h/D_1 < 1.25$, where the onset of separation in crosswind will be strongly affected by the presence of the ground plane.

The reattachment condition is insensitive to the ground clearance, except at very low values where the flow becomes more reluctant to reattach. This implies that once the flow has separated the presence of the ground has a reduced effect on the internal flowfield.

Figure 9 shows how the separation and reattachment angles vary with Reynolds number with all other experimental variables fixed. Below a Reynolds number of 10^5, the flow is always separated. Between Reynolds numbers of 10^5 and 1.5×10^5, the flow only reattaches with a wind direction parallel to the centerline. The separation angle increases rapidly, and at Reynolds numbers above 2×10^5 the flow separation and reattachment angles are fairly constant, but increasing slowly.

Figure 10 shows the effect of the fan operating condition on the separation hysteresis. The crosswind angle at separation is

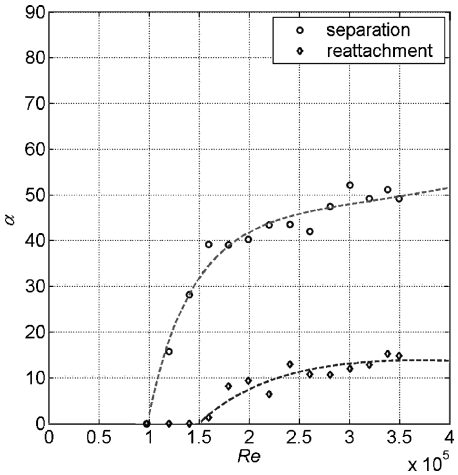

Fig. 9 Hysteresis map showing the effects of inlet Reynolds number: $h/D_1 = 1$, $L_q/D_1 = 3$, and $\phi = 0.62$.

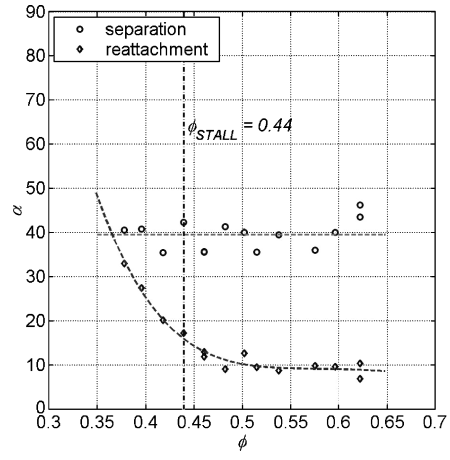

Fig. 10 Hysteresis map showing the effects of the downstream fan flow coefficient: $Re = 3 \times 10^5$, $L_q/D_1 = 3$, and $h/D_1 = 1$.

insensitive to the fan flow coefficient. This is presumably because the fan does not influence the pressure gradients around the inlet lip. However, a large effect is seen for the reattachment angle. As the fan flow coefficient is reduced, the inlet flow reattaches sooner. In fact, there is a point where the hysteresis is almost entirely eliminated, and this is not seen on any of the other plots. The same experiment was performed at different values of ground clearance, and the effect of the fan was found to be similar.

The mechanism by which the fan influences the flow reattachment is a subject for further work. A fan would typically be expected to have a smaller effect on a distorted inlet flowfield as stall is approached because the gradient of the pressure rise characteristic is reduced at lower flow coefficients (see Longley and Greitzer[16]). However, in this case the reverse is true, and the fan seems to have a greater effect on reattachment when at or beyond the stall boundary. Unsteady pressure measurements made upstream of the fan show that for low values of fan flow coefficient the pressure fluctuations become significant, and this could be an indication of the mechanism that is causing early reattachment. Further research is therefore recommended in the area of determining how a fan at or beyond instability interacts with separated inlet flow.

V. Discussion

The present paper has presented a complete, self-contained study of intake separation hysteresis. The authors believe that the results are applicable to full-scale engine intakes, but some further discussion of this point is merited.

The model rig nacelle separates at crosswind angles that are typical for the Reynolds number of the experiments. The low Reynolds numbers used are a fundamental consequence of the model rig experiments, and equivalent tests at full-scale Reynolds number were not possible. As the Reynolds number increases, the flow becomes gradually more resistant to separation (see Fig. 9). This trend continues up to full-scale Reynolds numbers in the range 10^6 to 10^7, as shown by Younghans et al.[17] This suggests that although the flow angles at separation are low for the model rig the trends in how the separation conditions vary with other experimental variables should apply at higher Reynolds number.

Across the complete range of Reynolds numbers, separation of the flow entering an intake operating within a crosswind is a result of the same effect: overspeed of the flow around the inlet lip leading to an increased adverse pressure gradient. For the current study, we are primarily interested in how the intake performance in uniform, steady flow relates to that within natural wind (see Hall and Hynes[3]). Thus the absolute values of the conditions at separation are not critical.

For a full-scale intake, the Mach number of the flow in the far-field wind can be as low as 0.02, whereas around the lip of the nacelle it can be higher than 1.5. This introduces significant compressibility effects into the flowfield. In particular, the flow separation will often be caused by shock-boundary-layer interaction, whereas for the model rig it is thought to be the bursting of a laminar separation bubble. However, both mechanisms are initiated by increased aerodynamic loading of the inlet lip in crosswind, and downstream of the separation point the flow is comparable: the separation forms a region of low total pressure fluid that convects downstream towards the engine face. The size of the separation produces levels of distortion that are similar in both cases. Compressibility can, therefore, affect the separation hysteresis, but it will not eradicate it. There are several examples of transonic flowfields that exhibit hysteresis, and shock waves are a source of irreversibility that have been shown to promote nonunique behavior.

In steady conditions for an engine, an engine fan is known to reduce the size of a separated region but to have little effect on the lip pressure field (see Motycka[18]). Thus the fan has an effect on the internal flowfield post separation, but it has little influence on when the flow separates. This is also true for the model rig.

The fan operating condition used for most of the model rig experiments is much further from stall than would be typical of a full-scale engine fan. The poststall behavior of a full-scale engine is expected to be quite different to that of the model rig, and further research is required to examine the coupling between intake separation and a stalled fan. It would be particularly interesting to determine whether an engine fan can affect flow reattachment in a similar way to that shown by Fig. 10.

VI. Conclusions

An extensive series of tests have been completed with a model fan and intake rig operating in uniform, low-turbulence crosswinds. The effects of the rig Reynolds number, fan flow coefficient, stream-tube contraction ratio, wind direction, and ground clearance have been assessed. Separation hysteresis was found to be of fundamental importance to the rig behavior, and a detailed investigation of the separation and reattachment behavior has been completed.

The far-field flow direction α and its variation are the main factors determining whether the inlet flow is separated or attached. When the flow is attached, increasing the wind angle increases the peak lip loading bringing the flowfield closer to separation. Once the flow is separated, the size of the distortion presented to the fan face grows as the angle of the wind increases. If the wind angle is reduced after the flow has separated, reattachment occurs at a much lower angle than that required for separation. The separation and reattachment angles are unique functions of the other experimental variables.

The stream-tube contraction ratio L_q/D_1 determines the extent of the engine influence into the far field. When the wind direction is parallel to the engine centerline, the peak aerodynamic loading on the inlet increases with stream-tube contraction. However, when there is a crosswind component, the rate of change in lip loading with respect to wind angle decreases with increasing L_q/D_1. These trends agree with the available data on high-speed inlets. The overall effect for the model rig is that when the stream-tube contraction ratio increases the wind angle required for separation increases, and the angle required for reattachment decreases. Thus, the separation hysteresis increases with stream-tube contraction ratio.

The rig has shown that for the nondimensional ground clearances typical of jet engines, as h/D_1. decreases the tendency for the flow to separate rises. High-speed nacelles exhibit the same trend (see Quemard et al.[11]). The proximity of the ground promotes separation in two ways: first, it redistributes the pressure field around the nacelle circumference, increasing the lip loading towards the top; and second, it causes the flow drawn into the intake to be less uniform. Flow drawn from close to the ground has lower total pressure, and the presence of an inlet vortex introduces swirl. It is thought that the more three-dimensional and nonuniform internal flowfield is less stable and more easily separated by adverse pressure gradients. If the ground clearance is sufficient for the entire capture stream tube to be clear of the ground, then the internal flowfield is considerably more stable, and the wind direction required for separation is much greater.

The fan has negligible effect on the onset of inlet flow separation but a strong influence on the reattachment condition. As the fan flow coefficient reduces, the inlet flow reattaches at a greater wind angle. This effect of the fan on the flow reattachment is thought to be the result of interaction between the separated portion of the internal flowfield and the part of the fan annulus that is operating at a reduced flow coefficient, on the stalled characteristic. The unsteadiness generated by the interaction is believed to encourage entrainment into the separated shear layer thus promoting reattachment.

Although the experiments were performed at low Reynolds number and Mach number, the results demonstrate behavior that we believe is applicable to full-scale engine intakes. In particular, the tests indicate the effects of separation hysteresis should be accounted for in all tests and calculations of intakes in crosswind. The observed effects of the fan operating point and the position of the ground plane highlight the need for intake tests and calculations to include a ground plane and a model of any downstream turbomachinery.

Appendix: Uncertainty Analysis

The error in an experimental variable that is derived from a combination of measurements, such as stream-tube contraction or Reynolds number, has to be determined using uncertainty analysis. For this paper, the partial differential method described in Abernathy et al.[19] was applied. This technique calculates the relative influence

of each raw measurement on the parameter of interest. The total measurement error is then the sum of the rms of the influences of each measurement.

The stream-tube contraction ratio can be expressed in terms of quantities that have been measured directly using the following equation (also known as a data-reduction equation):

$$\frac{L_q}{D_1} = \sqrt{\frac{\dot{m}_f}{\rho_\infty V_\infty D_1^2}} = \sqrt{\frac{\rho_\infty A_f U_f \phi_f}{\rho_\infty V_\infty D_1^2}} = \sqrt{\frac{A_f \bar{r}_f}{D_1}} \sqrt{\frac{\Omega_f \phi_f}{V_\infty}} \quad \text{(A1)}$$

The fan area, mean fan radius, and inlet highlight diameter are all geometric quantities that are determined with high accuracy and are therefore assumed to contribute minimal error. Thus the uncertainty equation for the stream-tube contraction can be written as

$$\frac{\delta(L_q/D_1)}{L_q/D_1} = \left\{ \left[\frac{\partial(L_q/D_1)}{\partial \Omega_f} \delta\Omega_f \right]^2 + \left[\frac{\partial(L_q/D_1)}{\partial \phi_f} \delta\phi_f \right]^2 + \left[\frac{\partial(L_q/D_1)}{\partial V_\infty} \delta V_\infty \right]^2 \right\}^{\frac{1}{2}} \Bigg/ \sqrt{\frac{\Omega_f \phi_f}{V_\infty}} \quad \text{(A2)}$$

Replacing the partial derivatives with quantities that can be evaluated, the uncertainty in the stream-tube contraction ratio can be determined using the following formula:

$$\frac{\delta(L_q/D_1)}{L_q/D_1} = \left\{ \left(\frac{1}{2} \Omega_f^{-\frac{1}{2}} \delta\Omega_f \sqrt{\frac{\phi_f}{V_\infty}} \right)^2 + \left(\frac{1}{2} \phi_f^{-\frac{1}{2}} \delta\phi_f \sqrt{\frac{\Omega_f}{V_\infty}} \right)^2 + \left(-\frac{3}{2} V_\infty^{-\frac{3}{2}} \delta V_\infty \sqrt{\Omega_f \phi_f} \right)^2 \right\}^{\frac{1}{2}} \Bigg/ \sqrt{\frac{\Omega_f \phi_f}{V_\infty}} \quad \text{(A3)}$$

The fan speed Ω_f was recorded using an optical sensor that receives a once-per-rev signal from the model rig fan, and a strobe light showed the accuracy of this measurement to be $\pm 0.1\%$. The fan flow coefficient ϕ_f was determined from the throttle calibration, and, as discussed in Sec. II, the error in this is expected to be $\pm 2\%$. The characteristic mean far-field wind speed V_∞ was determined using a rotating vane anemometer positioned at the side of the wind tunnel upstream of the wind-tunnel turntable. This measurement was corrected to account for the fact that the wind speed in front of the rig was found to be less than at the measurement point. By comparison with a sensitive differential pressure measurement method, the anemometer output was found to be accurate to within $\pm 4\%$. The overall uncertainty in stream-tube contraction ratio was determined using Eq. (A3), with the preceding uncertainties combined with nominal values for the measured quantities. This gave an overall error of $\pm 6\%$.

The data-reduction equation for the intake Reynolds number is derived as follows:

$$Re = \frac{\dot{m}_f}{\mu D_1} = \frac{\rho_\infty A_f U_f \phi_f}{\mu D_1} = \frac{p_\infty}{R T_\infty} \frac{A_f U_f \phi_f}{\mu D_1} = \frac{A_f \bar{r}_f}{\mu D_1 R} \frac{p_\infty \Omega_f \phi_f}{T_\infty} \quad \text{(A4)}$$

Thus, the uncertainty in Reynolds number is determined using the same process as shown for the stream-tube contraction ratio. This leads to the following relationship:

$$\frac{\delta Re}{Re} = \left[\left(\frac{\Omega_f \phi_f}{T_\infty} \delta p_\infty \right)^2 + \left(\frac{p_\infty \phi_f}{T_\infty} \delta\Omega_f \right)^2 + \left(\frac{p_\infty \Omega_f}{T_\infty} \delta\phi_f \right)^2 + \left(-\frac{p_\infty \Omega_f \phi_f}{T_\infty^2} \delta T_\infty \right)^2 \right]^{\frac{1}{2}} \Bigg/ \frac{p_\infty \Omega_f \phi_f}{T_\infty} \quad \text{(A5)}$$

The errors in the measurements of atmospheric pressure and temperature are relatively small, and in the preceding equation the error in the calibration of the rig throttle to calculate flow coefficient dominates. Thus the overall error in Reynolds number was calculated to be $\pm 2\%$.

Acknowledgments

The authors would like to acknowledge Fan Systems, Rolls-Royce plc for granting permission to C. A. Hall to carry out research at the Whittle Laboratory. They would also like to thank M. Whibley for the mechanical design and manufacture of the model rig. The use of the Osney wind tunnel was with the kind permission and assistance of C. Wood, R. Belcher, and M. Gamboa-Marrufo. The authors are grateful for financial support for this work from The Engineering and Physical Sciences Research Council and from Fan Systems, and the encouragement of A. Rae throughout the research is greatly appreciated.

References

[1]Freeman, C., and Rowe, A. L., "Intake Engine Interactions of a Modern Large Turbofan Engine," *Proceedings of the International Gas Turbine and Aero Engine Congress*, ASME Paper 99-GT-344, New York, June 1999.

[2]Hall, C. A., "Fan-Nacelle Interactions in Natural Wind," Ph.D. Dissertation, Dept. of Engineering, Univ. of Cambridge, Cambridge, England, UK, Oct. 2002.

[3]Hall, C. A., and Hynes, T. P., "Nacelle Interaction with Natural Wind Before Takeoff," *Journal of Propulsion and Power*, Vol. 21, No. 5, 2005, pp. 784–791.

[4]Day, I. J., and Cumpsty, N. A., "The Measurement and Interpretation of Flow Within Rotating Stall Cells in Axial Compressors," *Journal Mechanical Engineering Science*, Vol. 20, No. 2, 1978, pp. 101–114.

[5]Chang, P. K., *Separation of Flow*, Pergamon, Oxford, England, UK, 1970, pp. 452–530.

[6]Guzhavin, A. I., and Korobov, Y. P., "Hysteresis of Supersonic Flows with Separation," *Fluid Mechanics*, Vol. 19, No. 2, 1984, pp. 272–280.

[7]Newman, B. G., "Deflection of Plane Jets by Adjacent Boundaries: Coanda Effect," *Boundary Layer and Flow Control, Its Principles and Applications*, Vol. 1, Pergamon, Oxford, England, UK, 1961, pp. 232–264.

[8]Zanin, B. Y., "Hysteresis of a Variable-Velocity Flow About a Straight-Wing Model," *Journal of Applied Mechanics and Technical Physics*, Vol. 38, No. 5, 1997, pp. 725–727.

[9]Golovkin, M. A., Gorban, V. P., Simuseva, Y. V., and Stratonovich, A. N., "Flow over a Straight Wing Under Steady and Quasisteady External Conditions," *Fluid Mechanics—Soviet Research*, Vol. 17, No. 1, 1988, pp. 12–25.

[10]Horton, H. P., "A Semi-Empirical Theory for the Growth and Bursting of Laminar Separation Bubbles," *Aeronautical Research Council*, Vol. 1073, June 1969, pp. 1–44.

[11]Quemard, C., Garcon, F., and Raynal, J.-C., "High Reynolds Number Air Intake Tests in the ONERA F1 and S1MA Wind-Tunnels," TP 1996-213, ONERA, Toulouse, France, March 1996.

[12]Seddon, J., and Goldsmith, E. L., *Intake Aerodynamics*, 2nd ed., Blackwell Science, London, 1999, pp. 340–371.

[13]Wood, C., "The Osney Laboratory Environmental Wind Tunnel," *Journal of Industrial Aerodynamics*, Vol. 4, No. 1, 1979, pp. 43–70.

[14]Nangia, R. K., and Palmer, M. E., "On the Zero-Speed and Low-Speed Aspects of 3-D Aircraft Intakes," *Proceedings of the Royal Aeronautical Society*, London, Nov. 1998, pp. 2.1–2.14.

[15]McCroskey, W. J., Carr, L. W., and McAlister, K. W., "Dynamic Stall Experiments on Oscillating Airfoils," *AIAA Journal*, Vol. 14, No. 1, 1976, pp. 57–63.

[16]Longley, J. P., and Greitzer, E. M., "Inlet Distortion Effects in Aircraft Propulsion System Integration," *Steady and Transient Performance of Gas Turbine Engines*, edited by L. Fottner, AGARD LS-183, Cambridge, MA, May 1992, pp. 6.1–6.16.

[17]Younghans, J. L., Hoelmer, W., and Stockman, N. O., "Low Speed Effects of Reynolds Number and Lip Geometry on High Bypass Ratio Inlet Performance," AIAA Paper 82-0059, June 1982.

[18]Motycka, D. L., "Reynolds Number and Fan/Inlet Coupling Effects on Subsonic Transport Inlet Distortion," *Journal of Propulsion and Power*, Vol. 1, No. 3, 1985, pp. 229–234.

[19]Abernathy, R. B., Benedict, R. P., and Dowdell, R. B., "ASME Measurement Uncertainty," *Journal of Fluids Engineering*, Vol. 107, June 1985, p. 161.